

## Role of crustal fluid in triggering moderate to major earthquakes: evidence from aftershock data of two recent large tremors

\*Sushil Kumar<sup>1</sup>, Hiroaki Negishi<sup>2</sup>, Jim Mori<sup>3</sup>, and Tamao Sato<sup>4</sup>

<sup>1</sup>Wadia Institute of Himalayan Geology, Dehra Dun - 248 001, India

<sup>2</sup>National Research Institute for Earth Science and Disaster Prevention, Tenno-dai 3-1, Tsukuba, 305-0006, Japan.

<sup>3</sup>Disaster Prevention Research Institute, Kyoto University Gokasho, Uji, Kyoto 611-0011, Japan

<sup>4</sup>Hirosaki University, Bunkyo-cho 3, Hirosaki, 036-8561, Japan

(\*Email: sushilk@wihg.res.in)

### ABSTRACT

A number of models have been proposed for the role of fluids and high pore pressures in the mechanics of fault slip and the nucleation of earthquakes, e.g., dilatancy-diffusion, mineral dehydration, frictional heating, fluid pressure-activated fault valves and hydrofracturing, partially sealed fault zones, a spatially varying stress tensor without hydrofracturing, and fluid-involved weak and strong patch failures. In this study, the availability of fluid in the upper and lower crust was analysed carefully, as the fluid may be responsible for triggering large earthquakes. The anomalies observed in the three-dimensional tomographic images from the source regions of the 2001 Gujarat and 1995 Kobe earthquakes, obtained after inversion of aftershock data, can be attributed to the presence of the fluid. A tomographic inversion was also applied to the aftershock data from the 26 January 2001 Bhuj earthquake (Mw 7.7) in the state of Gujarat in western India. We used arrival times from 8,374 P and 7,994 S waves of 1,404 aftershocks recorded on 25 temporary seismic stations. It seems that the aftershock distribution corresponds to the high-velocity anomalies. Low P- to S-wave velocity ratio (Vp/Vs) anomalies are generally found at depths of 10 to 35 km, i.e. the depth range of the aftershock distribution. However, relatively high Vp/Vs and low Vs characterise the deeper region below the hypocentre of the mainshock, at depths of 35 to 45 km. This anomaly may be due to a weak fractured and fluid-filled rock matrix, which might have contributed to triggering this earthquake. This anomaly exists in the depth range of 35 to 45 km, and extends 10 to 12 km laterally. This earthquake occurred on a relatively deep and steeply dipping reverse fault with a large stress drop.

Similarly, the 17 January 1995 Kobe earthquake (M 7.2) in southwest Japan had a strike-slip focal mechanism and it caused a rupture at a 17 km depth. The Kobe mainshock hypocentre is located in a distinctive zone characterised by low P- and S-wave velocities and a high Poisson's ratio. This anomaly exists in a depth range of 16 to 21 km, and extends 15 to 20 km laterally. This anomaly can be attributed to a fluid-filled, fractured rock matrix that contributed to the initiation of the Kobe earthquake. The existence of fluids in and below the seismogenic layer may affect the long-term structural and compositional evolution of the fault zone, change the fault zone strength, and alter the local stress regime. These influences can be exerted through the physical role of fluid pressure and a variety of chemical effects, such as stress corrosion and pressure solution. These influences would have enhanced stress concentration in the seismogenic layer leading to mechanical failure of a strong asperity, and thus may have contributed to the nucleation of the Kobe earthquake.

The area of low Vs and high Vp/Vs values can be seen in a depth range of 35 to 45 km beneath the mainshock hypocentre. These features are very similar to the velocity anomaly also observed, in a depth range of 16 to 21 km, in the hypocentre region of the 1995 Kobe earthquake. Such an anomaly possibly indicates the existence of a fluid-filled, fractured rock matrix, which may have contributed to the initiation of large earthquakes. The fluid in a depth range of 35 to 45 km might have also triggered the 2001 Gujarat earthquake.

**Keywords:** Crustal fluid, 2001 Gujarat earthquake, 1995 Kobe earthquake, tomographic inversion, aftershock

**Received:** 22 August 2007; **revision accepted:** 27 November 2008

### INTRODUCTION

The 6 January 2001 Gujarat earthquake was a very large crustal tremor (Mw 7.7) in the state of Gujarat, India. This area is about 300 km south of the Himalayan Frontal Fault System, where the Indian and Eurasian plates collide, and about 400 km east of the junction between the Owens Fracture Zone, Makran Subduction Zone, and Chaman Fault. The

Kachchh Peninsula is one of the active seismic regions in India. Although this region is situated away from the active plate boundaries, there are large east–west trending compressional features that cross the Kachchh Peninsula (Fig. 1). These features, along with the current configuration of plate motions, suggest a north–south compressional stress field. This earthquake is one of the largest recent events in India, and brought serious damage to this region

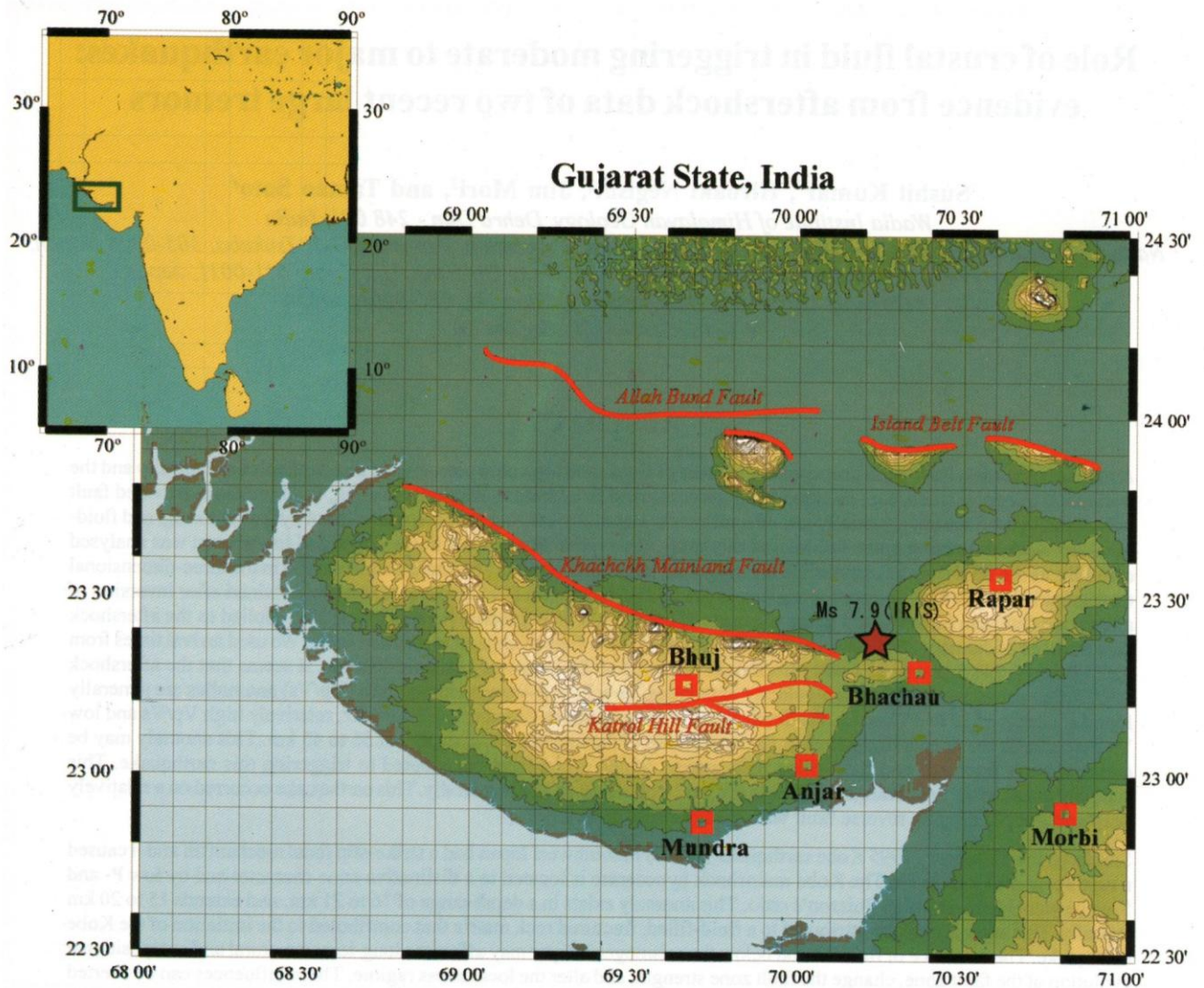


**Fig. 1:** Tectonic and regional map of the area of the 2001 Gujarat earthquake. Star denotes the epicentre of the 2001 earthquake determined by USGS. Faults are after Malik et al. (2000).

(over 20,000 deaths and over 400,000 destroyed buildings). This earthquake has unique features compared with the other large crustal earthquakes – the fault was rather deep and had a small area (Negishi et al. 2002). The moment magnitude of this earthquake ( $M_w$  7.7) is almost same as the recent earthquakes in Turkey and Taiwan, where large surface displacements of 5 to 8 m were observed (Youd et al. 2000; Ma et al. 2001). Surprisingly, the Gujarat earthquake did not have obvious surface displacements for the main fault, although there were some minor surface deformations attributed to the shaking effects.

In the present study, to investigate the velocity structure in the focal region of the 2001 Gujarat earthquake, we merged

three data sets collected by a number of agencies. We inverted the combined P and S arrival times and obtained a one-dimensional velocity model, station corrections, and hypocentres simultaneously. Then a three-dimensional P and S wave velocity structure was determined. We discuss the results in relation to the aftershock distribution and infer a possible mechanism for the generation of the 2001 Gujarat earthquake and 17 January 1995 Kobe earthquake, Japan. The variations in P-wave velocity ( $V_p$ ), S-wave velocity ( $V_s$ ), and  $V_p/V_s$  indicate the existence of highly fractured materials and fluid intrusion, which might have played the main role in triggering the devastating 2001 and 1995 Kobe earthquakes which had triggered due to similar anomaly fluid filled, fractured rock matrix at a depth of 16 to 21 km.

## TECTONIC SETTING

Gujarat is considered to be a stable continental region or a transition between stable continent and the active plate boundary. Even though the area is located away from the major plate boundaries, there are large east–west trending compressional features that cross the Kachchh Peninsula. The east–west structures include the Kachchh Mainland (uplifted and folded highlands of Mesozoic rocks), which is bordered on the north by the Kachchh Mainland Fault and on the south by the Katrol Hill Fault. To the north of the Kachchh Mainland is the broad Banni Plain and farther north are the large salt flats that comprise the Rann of Kachchh. In the Rann of Kachchh, there are several more east–west trending faults, including the Island Belt, Allah Bund, and Nagar Parkar faults. These features are thought to be reactivated Mesozoic rifts. The Kachchh rift basin was created in successive stages during the migration of the Indian plate after its break up from the Gondwana in late Triassic or early Jurassic. The onset of collision of India with the southern margin of Eurasia occurred in late Palaeocene–Eocene time, and following the collision, the Kachchh rift basin sustained stress reorientation. By late Miocene, the east–west trending Kachchh rift basin had formed and was being subjected to a north–south compressive stress field. The maximum horizontal stress that is responsible for current tectonic activity is oriented from N–S to NNE–SSW.

## SEISMICITY IN GUJARAT REGION

The Kachchh Peninsula has a history of active seismicity with several large damaging earthquakes ranging in magnitude from 6 to 7 over the last several hundred years. The largest known historical event in the region was the 1819 earthquake (M 7.5) that caused considerable damage in Bhuj and Anjar with 1500 casualties. This earthquake is notable for producing the Allah Bund (Wall of God) which is a 90 km long feature with vertical uplifts of up to 4.3 m. Rajendran and Rajendran (2001) claim that this feature is a composite scarp formed from a series of earthquakes. Prior to the 2001 Gujarat earthquake, the 1819 event was considered to be the fourth largest historical earthquake in a stable continental region. More recently the 1956 Anjar earthquake (Ms 6.1) occurred south of Bhuj with a thrust mechanism and compression in a north–northwest direction, similar to the 2001 event. Slightly further away, the 24 October 1969 Mt. Abu earthquake (M 5.3) to the northeast and the 23 March 1970 Broach earthquake (M 5.4) to the southeast, also had thrust mechanisms with north and north–northwest compression directions, respectively. There are also numerous other small events (M 3 to 5) scattered throughout the region.

## AFTERSHOCK DATA

After the occurrence of the 2001 Bhuj earthquake, several institutions installed temporary arrays of seismographs. We

merged these data sets recorded by the India–Japan team, National Geophysical Research Institute (India), and Center for Earthquake Research and Information, Memphis University (USA), to form a single synoptic aftershock database (Bodin et al. 2001). There were intermittent problems at several stations but we were able to use arrival times from 25 stations. The distribution of stations are shown in Fig. 2. We selected 1,404 earthquakes observed at more than five stations from the data set. For the present study, 8,374 P and 7,994 S wave arrival times of high quality were used. Zhao et al. (1996) analysed the 1995 Kobe earthquake. In this analysis they used 3203 Kobe aftershocks and 431 local micro earthquakes that generated 64,337 P and 49,200 S wave arrival times (Fig. 3).

## TOMOGRAPHY ANALYSIS

Since the tomographic results strongly depend on the initial model and hypocentres, firstly, we chose adequate initial P and S wave velocity models and good hypocentres before proceeding with the tomographic calculations. We applied the Joint Hypocentre Determination Method program coded by Kissling et al. (1994) to the data set and divided the crust and the uppermost mantle into 17 layers. The one-dimensional Vp and Vs models are shown in Fig. 4. There exist two low-velocity layers around the depths of 20 and 35 km, and high values of Vp/Vs can be seen between these layers. These depths correspond to the regions that are just above the Conrad and Moho depths (Gupta et al. 2001; Kumar et al. 2001), respectively. The high Vp/Vs values seem to be corresponding to the lower crust. Most of the aftershocks are located in this depth range, especially in the eastern part of the region.

The analytical techniques used here were the same as that of Zhao et al. (1992). This method determines both the P- and S-wave velocity structure and hypocentres simultaneously. The velocity structure is represented by discrete grid points and three-dimensional two-point ray tracing is employed. The grid interval is set to 0.05 degrees for horizontal, and the depth grid is set to the middle depth of each layer, as shown in Fig. 4.

Usually, damping parameters for tomographic inversion are often determined subjectively because we know nothing about these parameters *a priori*, but biased damping parameters may affect the absolute values of velocity perturbation. We applied the simplified cross validation (CV) technique (Inoue et al. 1990) to determine the optimum damping parameters in this study. The CV score is calculated with certain damping values in each iteration step and the optimum damping parameters and iteration number are determined by the values that produce the minimum score. The minimum CV score in this study is located at the point with values of 4%, 8%, and 10 iterations for the Vp-damping, Vs-damping, and iteration number, respectively.

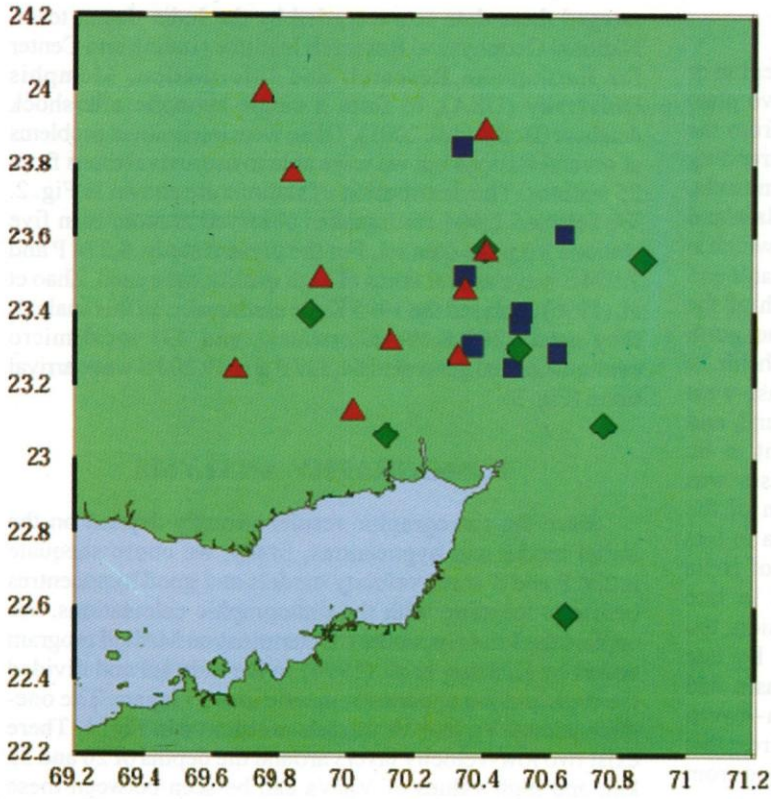


Fig. 2: Distribution of stations used in this study. There were the following three seismic arrays: operated by the India–Japan team (blue rectangle); National Geophysical Research Institute (green diamond); and Center for Earthquake Research and Information (CERI), Memphis University (red triangle).

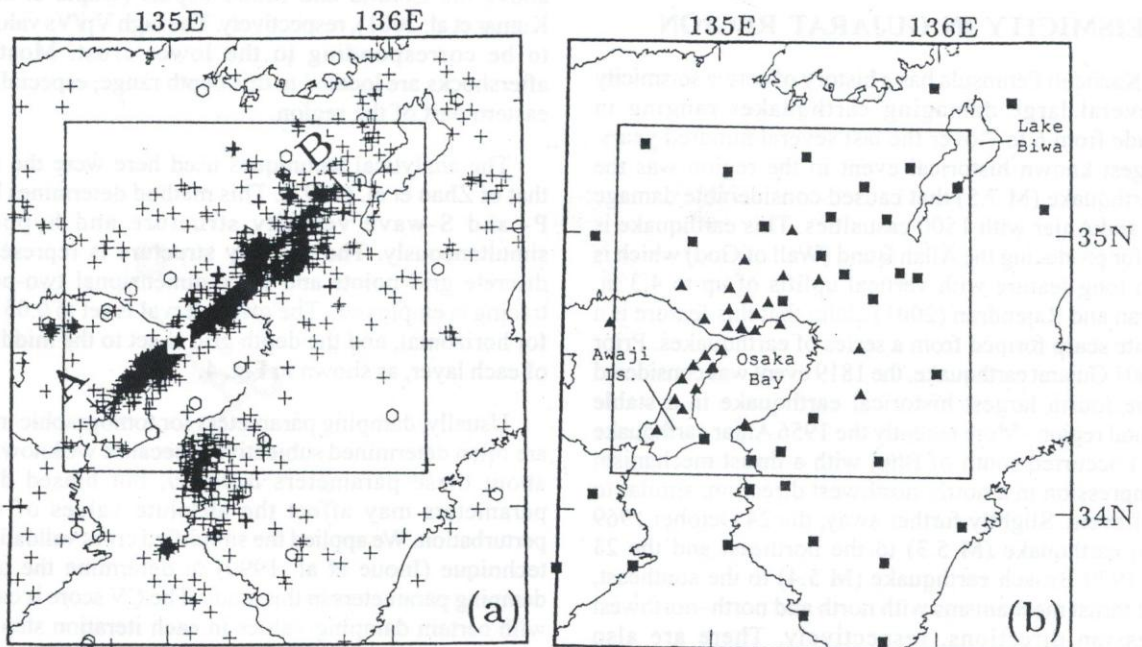


Fig. 3: (a) Epicentral distribution of the 3634 earthquakes used in the Kobe aftershock analysis. Crosses denote the earthquakes that occurred after 17 January 1995; most of these were aftershocks ( $M$  between 1.5 and 3.0) of the  $M$  7.2 Kobe earthquake (star symbol) along the fault zone (parallel to cross-section line A–B). Circles denote earthquakes that occurred from January 1990 to December 1994, with  $M$  between 1.8 and 4.0. The Cross-section along A–B is shown in Fig. 7. (b) Distribution of seismic stations that were set up following the Kobe main shock. Solid squares denote permanent stations. Solid lines represent the surface traces of the Nojima, Suma, and Suwayama faults.

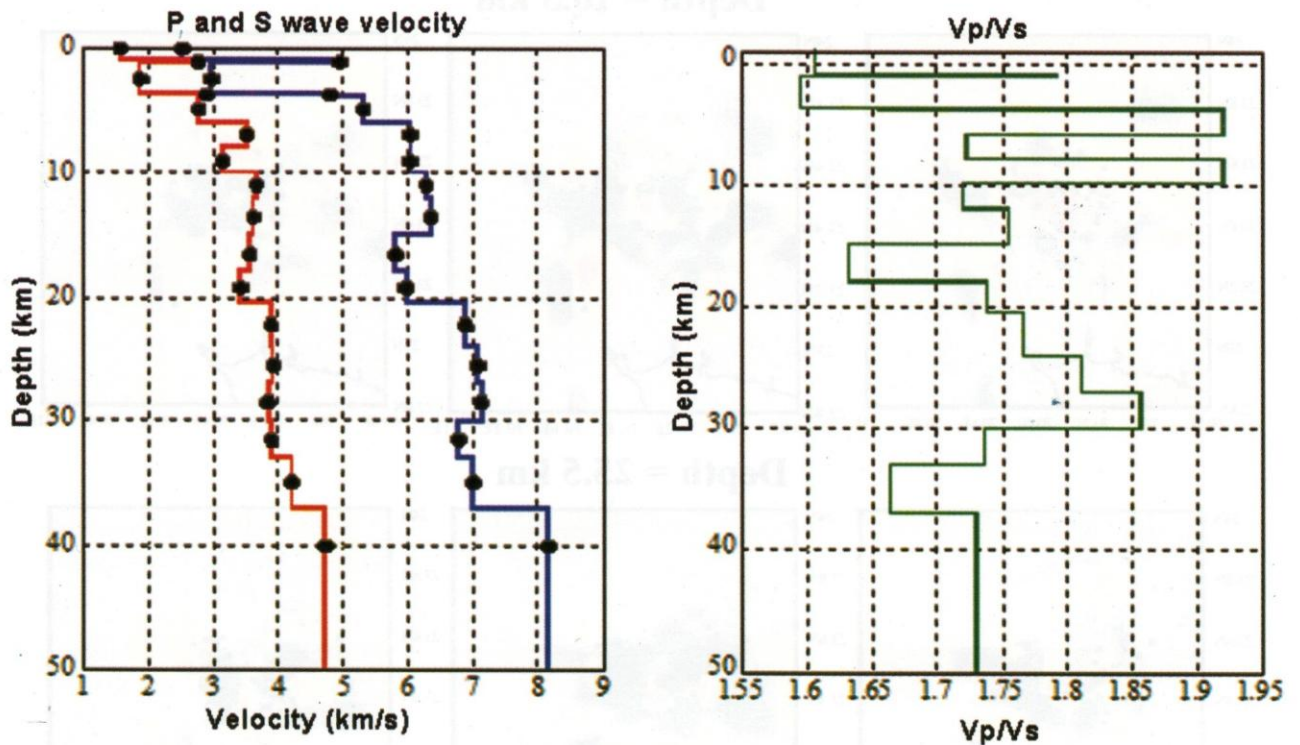


Fig. 4: The one-dimensional velocity structure used as the initial model for the tomographic study. This model was determined by the joint hypocentre determination method. The distribution of grid nodes for the tomographic inversion is shown as circles.

In the study of Kobe earthquake, Zhao et al. (1996) used the tomographic method of Zhao et al. (1992) to determine the three dimensional (3D) P- and S-wave velocity ( $V_p$ ,  $V_s$ ) and  $\delta$  distribution maps in the source area.

## RESULT AND DISCUSSION

The results of the fractional P and S waves velocity structure and  $V_p/V_s$  distribution at several depths are shown in Fig. 5. The vertical sections of the velocity structure are shown in Fig. 6. These sections are oriented in the N12°W direction, which is inferred to be close to the directions perpendicular to the fault from the mainshock focal mechanism (Kikuchi and Yamanaka, personal comm.). Velocity perturbations are given relative to the one-dimensional velocity (Fig. 4) in each layer. Significant variations in the velocity (up to 6%) and  $V_p/V_s$  (up to 8%) are revealed in the surrounding area. Generally, the low  $V_p/V_s$  region corresponds to the high seismicity region, close to the fault plane, for the western part of the aftershock area. On the other hand, where aftershocks are concentrated in the eastern region, there are relatively high  $V_p/V_s$  values. In the areas very close to the mainshock hypocentre, there are low  $V_p$ , low  $V_s$ , and high  $V_p/V_s$  values. This might be an expression of the existences of highly fractured materials and fluid intrusion. The area of low  $V_s$  and high  $V_p/V_s$

values can be seen in a depth range of 35 to 45 km beneath the mainshock hypocentre. Kayal et al. (2002) used 331 events recorded at least four stations. These features are very similar to the velocity anomaly in the hypocentre region of the 1995 Kobe earthquake (Zhao et al. 1996). Such an anomaly possibly indicates the existence of a fluid-filled, fractured rock matrix, which may contributed to the initiation of large earthquakes (Zhao and Negishi 1998). The fluid in a depth range of 35 to 45 km might have triggered the 2001 Gujarat earthquake. Our location of aftershocks indicates a plane that dips towards the south at an angle of about 50°, which is interpreted to be the fault plane of the mainshock. Sibson (1989) argues that such a dip angle is too steep to slip as a reverse fault because Byerly friction locks it up with increasing stress. An intrusion of over-pressured fluid can solve this problem. Usually, the faulting extent of an earthquake that occurs in the continental crust is limited to portions shallower than 15 to 20 km (Ito 1990). The rheology, which can be inferred from the three-dimensional velocity structure of this study, should contribute to the understanding of the causes of this very damaging earthquake.

Similarly, in the 17 January 1995 Kobe earthquake (M 7.2) in southwest Japan, rupture started at a 17 km depth, through a strike-slip focal mechanism. The Kobe mainshock hypocentre is located in a distinctive zone characterised by low P- and S-wave velocities and a high Poisson's ratio

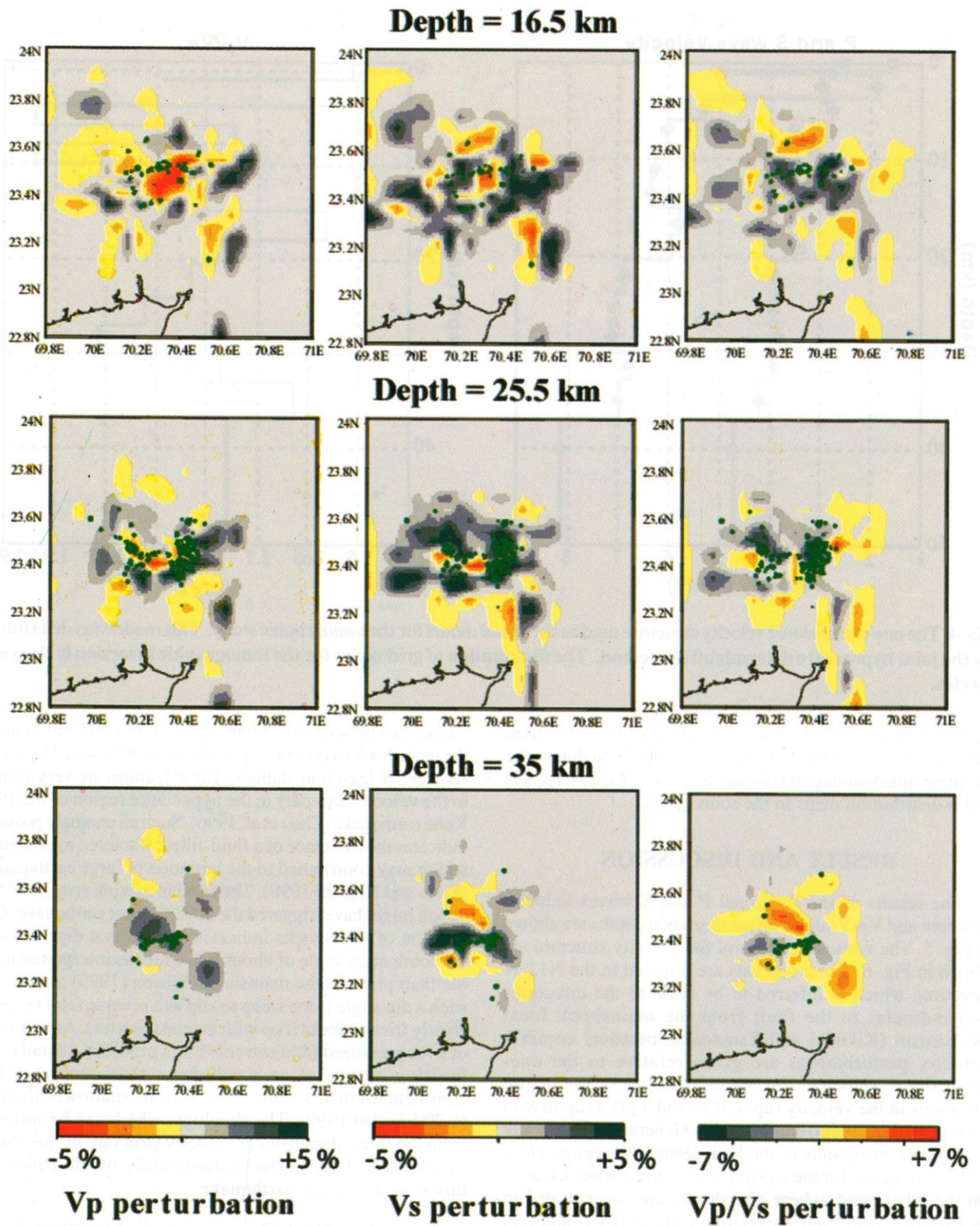


Fig. 5: Map views of the obtained P-wave velocity perturbation, S-wave velocity perturbation, and Vp/Vs perturbation. Layers corresponding to three depths around the mainshock hypocentre are shown. Aftershocks occurring in each depth range are also shown.

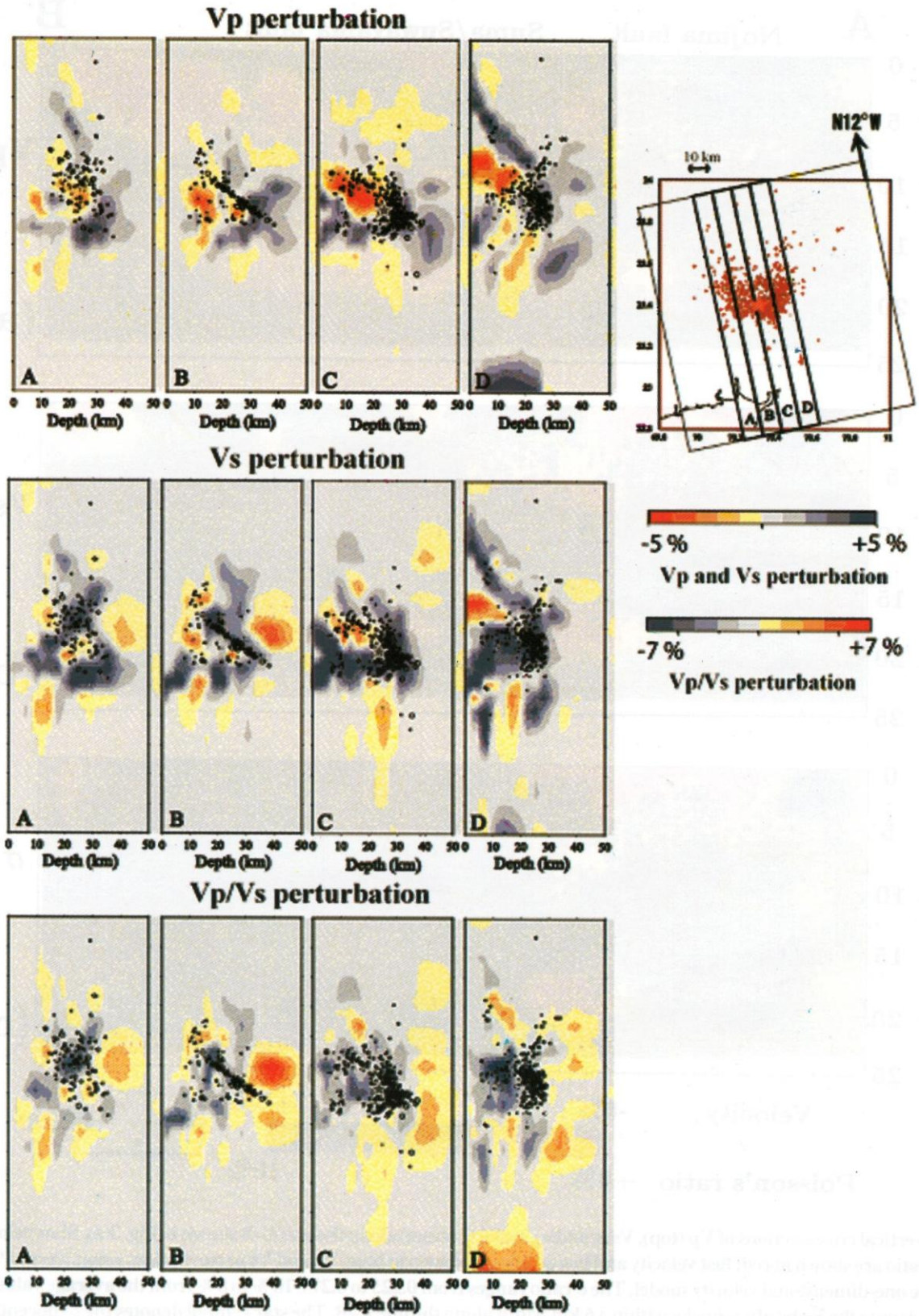


Fig. 6: P- and S-wave velocity and Vp/Vs perturbations in cross-sections perpendicular to the fault strike. Aftershock locations are also shown.

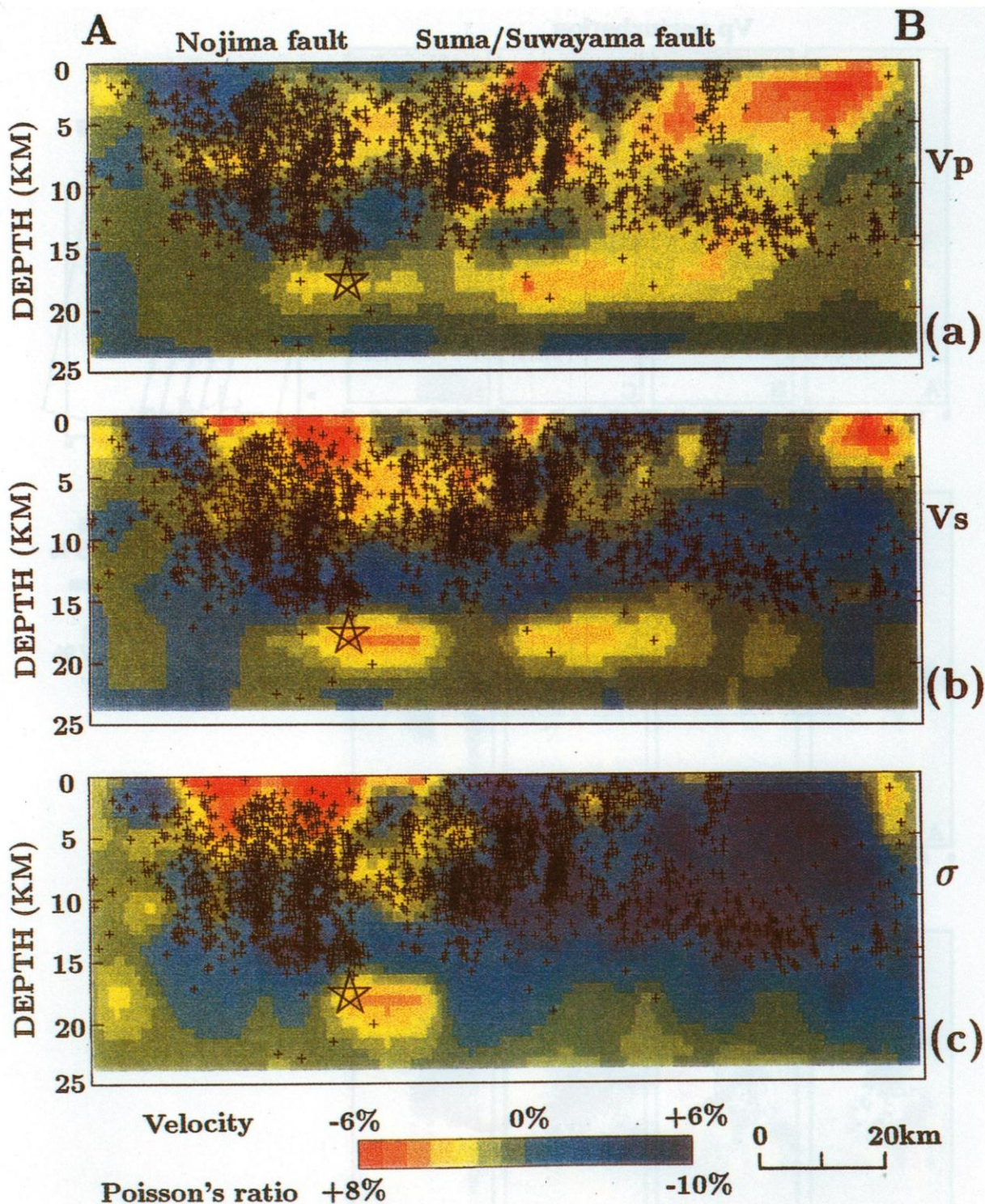


Fig. 7: Vertical cross-sections of  $V_p$  (top),  $V_s$  (middle), and  $\sigma$  (bottom) along the line A-B shown in Fig. 3(a). Slow velocity and high  $\sigma$  ratio are shown in red; fast velocity and low  $\sigma$  ratio are shown in blue.  $V_p$  and  $V_s$  perturbations range from -6% to 6% from the one-dimensional velocity model. The  $\sigma$  ratio ranges from 0.225 to 0.27 (-10% to 8% from the average value). Small crosses denote the Kobe aftershocks within a 6 km width along the line A-B. The star symbol denotes the hypocentre of the Kobe mainshock; its focal depth is 17.7 km.



(Fig. 7). This anomaly exists in a depth range of 16 to 21 km, and extends 15 to 20 km laterally. This anomaly may be due to a fluid-filled, fractured rock matrix that contributed to the initiation of the Kobe earthquake. Gupta et al. (1996) studied the hypocentral region of the Latur earthquake (Mw 6.1) triggered on 30 September 1993. They carried out the MT soundings, which provided an evidence for shallow fluid-filled zone in the upper crust below the hypocentral region of the Latur earthquake. The existence of highly conductive fluid-filled layer enhances the stress concentration in the uppermost part of the crust leading to mechanical failure.

The existence of fluids in and below the seismogenic layer may affect the long-term structural and compositional evolution of the fault zone, change the fault zone strength, and alter the local stress regime. These influences can be exerted through the physical role of fluid pressure and a variety of chemical effects, such as stress corrosion and pressure solution. These influences would have enhanced stress concentration in the seismogenic layer leading to mechanical failure of a strong asperity, and thus may have contributed to the nucleation of the Kobe earthquake. A number of models have been proposed on the role of fluids and high pore pressures in the mechanics of fault slip and the nucleation of earthquakes, e.g., dilatancy-diffusion, mineral dehydration, frictional heating, fluid pressure-activated fault valves and hydrofracturing, partially sealed fault zones, a spatially varying stress tensor without hydrofracturing, and fluid-involved weak and strong patch failures. The availability of fluid in the upper and lower crust should be analysed carefully, which may be responsible in triggering major to great earthquakes.

## CONCLUSIONS

We investigated the velocity structure of the source region of the 2001 Gujarat, India, earthquake. A one-dimensional inversion process and a three-dimensional tomographic analysis were applied to the aftershock data. The resultant velocity structure shows that the aftershock distribution occurred mainly in the areas of high velocity. However,  $V_p/V_s$  anomalies show different correlations in different regions. The area of high seismicity along a lineament (equivalent to the fault plane) in the western region has low values of  $V_p/V_s$ , while in the eastern region, the area with many aftershocks in the lower crust around the mainshock hypocentre has a high value of  $V_p/V_s$ . The area very close to the mainshock hypocentre has low  $V_p$ , low  $V_s$ , and high  $V_p/V_s$  values. This may be an indication of the existence of highly fractured materials and fluid intrusion, which might have triggered this devastating earthquake. The tomographic images showed pockets of fluids that were collecting in underground fault-line gaps. The trapped fluid acted as a "lubricant" for further fault-line slips and subsequent earthquakes. Similarly, the 1995 Kobe earthquake (M 7.2) in Japan exhibited a strike-slip focal mechanism. A distinctive anomaly identified is characterised by low P- and

S-wave velocities and a high Poisson's ratio. This anomaly exists in a depth range of 16 to 21 km, extends 300 km laterally, and indicates a fluid-filled fractured rock matrix that contributed to the initiation of the Kobe earthquake. The 30 September 1993 Latur, India, earthquake also was triggered by a shallow fluid-filled zone in the upper crust, below the hypocentral region. Our results provide information for imaging the source area and understanding the rheological causes of this earthquake. Present investigation is also important for evaluating the seismic hazard in continental areas.

## REFERENCES

- Bodin, P., Horton, H., Mandal, P., Rastogi, B. K., Sato T., Johnston, 2001, Multiagency database for Bhuj aftershocks. Abstracts of the International conference on seismic hazard with particular reference to Bhuj earthquake of January 26, 2001, pp. 107–108.
- Gupta, H. K., Rao, P., Rastogi, B. K. and Sarkar, D., 2001, The deadliest intraplate earthquake: Perspectives. *Science*, v. 291, pp. 2101–2102.
- Gupta, H. K., Sarma S. V. S., Harinarayana, T., Virupakshi, G., 1996, Fluids below the hypocentral region of Latur earthquake, India: Geophysical indicators. *Geophys. Res. Lett.*, v. 23, No. 13, Pages 1569–1572.
- Inoue, H., Fukao, Y., Tanabe, K. and Ogata, Y., 1990, Whole mantle P-wave travel time tomography. *Phys. Earth Planet. Inter.*, v. 59, pp. 294–328.
- Ito, K. 1990, Regional variation of the cutoff depth of seismicity in the crust and their relation to heat flow and large inland-earthquakes. *Jour. Phys. Earth*, v. 38, pp. 223–350.
- Kayal, J. R., Zhao, D., Mishra, O. P., De, R., and Singh, O. P., 2002, The 2001 Bhuj earthquake: tomographic evidence for fluids at the hypocenter and its implications for rupture nucleation. *Geophys. Res. Lett.*, v. 29(24), 2152, doi: 10.1029/2002GL015177.
- Kissling, E., Ellsworth, W. L., Eberhart-Phillips, D., and Kradolfer, U., 1994, Initial reference models in local earthquake tomography. *Jour. Geophys. Res.*, v. 99, pp. 19635–19646.
- Kumar, M. R., Saul, J., Sarkar, D., Kind, R., and Shukla, A. K., 2001, Crustal structure of the Indian shield: New constraints from teleseismic receiver functions. *Geophys. Res. Lett.*, v. 28, pp. 1339–1342.
- Ma, K. F., Mori, J., Lee, S. J., and Yu, S. B., 2001, Spatial and temporal distribution of slip for the 1999 Chi-Chi, Taiwan, earthquake. *Bull. Seismol. Soc. Am.*, v. 91, pp. 1069–1087.
- Malik, J. N., Sohoni, P. S., Merh, S. S., Karanth, R. V., 2000, Paleoseismology and neotectonics of Kachchh, western India, Active fault research of the New Millennium. Proceedings of the Hokudan International Symposium and School on Active Faulting (Ed. Okumura, K., Goto, H., and Takada, K.), pp. 251–259.
- Negishi, H., Mori, J., Sato, T., Singh, R., Kumar, S., and Hirata, N., 2002, Size and orientation of the fault plane for the 2001 Gujarat, India earthquake (Mw 7.7) from aftershock observations: A high stress drop event. *Geophys. Res. Lett.*, v. 29, No. 20, 1949, doi:10.1029/2002GL015280.
- Rajendran, C. P. and Rajendran, K., 2001, Characteristics of deformation and past seismicity associated with the 1819 Kutch

- earthquake, northwestern India. Bull. Seismol. Soc. Am., v. 91, pp. 407-426.
- Sibson, R. H., 1989, Earthquake faulting as a structural process. Jour. Struct. Geol., v. 11, pp. 1-14.
- Youd, T. L., Bardet, J. P., and Bray, J., 2000, Kocaeli, Turkey, earthquake of August 17, 1999 Reconnaissance Report. Earthquake Spectra, Supplement A to v. 16, pp. 1-461.
- Zhao, D., Hasegawa, A. and Horiuchi, S., 1992, Tomographic imaging of P and S wave velocity structure beneath northeastern Japan. Jour. Geophys. Res., v. 97, pp. 19909-19928.
- Zhao, D., Kanamori, H., Negishi, H. and Wiens, D., 1996, Tomography of the source area of the 1995 Kobe earthquake: Evidence for fluids at the hypocenter? Science, v. 274, pp. 1891-1894.
- Zhao, D. and Negishi, H., 1998, The 1995 Kobe earthquake: Seismic image of the source zone and its implication for the rupture nucleation. Jour. Geophys. Res., v. 103, pp. 9967-9986.